Original Article

Optimal scanning parameters of lumbar bone density measured by fast kilovoltage-switching dual-energy computed tomography (DECT)

Qiushi Yang, Zeguo Wang, Heli Han, Han Zhang, Wanjiang Yu

Department of Radiology, Qingdao Hospital, University of Health and Rehabilitation Sciences (Qingdao Municipal Hospital), Qingdao, China

Contributions: (I) Conception and design: W Yu, Q Yang; (II) Administrative support: W Yu; (III) Provision of study materials or patients: Z Wang; (IV) Collection and assembly of data: Z Wang, H Han, H Zhang; (V) Data analysis and interpretation: Q Yang, Z Wang; (VI) Manuscript writing: All authors; (VII) Final approval of manuscript: All authors.

Correspondence to: Wanjiang Yu, PhD. Department of Radiology, Qingdao Hospital, University of Health and Rehabilitation Sciences (Qingdao Municipal Hospital), 51 Donghai Middle Road, Shinan District, Qingdao 266071, China. Email: 18661678281@163.com.

Background: The technological innovation of fast kilovoltage (KV)-switching dual-energy computed tomography (DECT) has enabled the accurate measurement of vertebral bone density; however, it does not account for the effects of abdominal fat and ribs on the vertebral body. In our study, a European spine phantom (ESP) was used to establish an abdominal phantom for normal weight and obese people, and to explore the best scanning parameters for DECT to measure the bone mineral density (BMD) of the human lumbar spine.

Methods: Revolution CT was used to conduct energy spectrum scanning for each body mode. A total of 20 sets of energy spectrum scans was conducted and each set of conditions was scanned 10 times. The data conformed to a normal distribution, and the differences between the measured and actual values of ESP L1–3 vertebrae were compared using a one-sample *t*-test, and quantitative data were described by $\bar{x}\pm s$. A P value <0.05 was considered statistically significant. Relative error (RE) and root mean square error (RMSE) of BMD measurements were calculated for different scanning conditions in normal and obese populations.

Results: When simulating the upper abdominal condition (L1–2 level, fat area 140 cm^2, with rib influence) in a normal weight population, there was no statistical difference (P>0.05) in BMD measurements for each vertebra at 0.8 s/rotation (rot) with different tube currents, the smallest RE at 0.8 s/rot, 190 mA condition, and the smallest RMSE for L1 and 2 vertebral BMD measurements at 190 mA; when simulating the abdominal condition at the L4 level in a normal weight population (fat area of 240 cm^2, no rib influence), there were no statistical differences between the measurements at 0.8 s/rot, 190 and 275 mA conditions (P>0.05), and the RE and RMSE in the 190 mA condition was smaller than that in the 275 mA condition. Simulating the upper abdominal condition in the obese population (L1–2 level, fat area 340 cm^2, with rib influence), there were no statistical difference between the measurements in the 0.8 s/rot, 315 and 355 mA conditions (P>0.05), the RE and RMSE in the 315 mA condition was less than those in the 355 mA; simulated obese abdominal condition at the L4 level in the population (fat area 450 cm^2, no rib influence) resulted in 0.8 s/rot, no statistical difference in measurements between 315 mA (P>0.05), RE in 315 mA conditions were L1: 3.75%, L2: –1.06%, L3: 0.42%, and the RMSE under 315 mA condition were L1: 2.13, L2: 1.21, L3: 1.66.

Conclusions: When using Revolution CT to measure lumbar spine bone density, 0.8 s/rot at 190 mA may be the best scanning parameter for a normal weight population, and 0.8 s/rot at 315 mA may be the best scanning parameter for an obese population.

Keywords: Quantitative computed tomography (QCT); dual-energy computed tomography (DECT); bone mineral density (BMD); osteoporosis

Submitted Dec 20, 2023. Accepted for publication Apr 15, 2024. Published online May 24, 2024.
doi: 10.21037/qims-23-1741
View this article at: https://dx.doi.org/10.21037/qims-23-1741

Introduction

Osteoporosis is a systemic osteopathy characterized by decreased bone mass and damaged bone microstructure, leading to increased bone fragility and fracture susceptibility (1). These fractures lead to high morbidity and mortality without timely treatment. Therefore, the early diagnosis and prevention of osteoporosis is very important.

Bone mineral density (BMD) is considered a major indicator for monitoring osteoporosis and estimating fracture risk, therefore, accurate measurement of BMD is very important. Dual-energy X-ray densitometry (DXA) and quantitative computed tomography (QCT) are considered reference standards for measuring BMD (2). DXA is widely used due to its low cost and low radiation dose and provides accurate BMD measurements *in vitro* (e.g., vertebral body in uniform fluid) (3). However, the measurements have difficulties while meeting vascular calcification, scoliosis, and spinal degeneration which can generate inaccurate diagnoses. In addition, DXA measures the entire vertebral BMD and cannot distinguish cortical bone and cancellous bone (4,5). QCT is a quantitative technique to measure volumetric bone mineral density (vBMD), regardless of bone size and shape, and there is solid evidence supporting its clinical value (6). However, studies have shown that abdominal fat content and spinal marrow fat content can affect the measurement of vertebral BMD by QCT (7-12), especially patients whose BMD <80 mg/cm^3. Since QCT was performed by using a compound to make standard phantom of equivalent water and bone, the phantom and the measured part were scanned synchronously, and then transformed into vBMD by linear regression with X-ray attenuation. The absorption and attenuation curve of abdominal fat to X-ray is arcuate, that is to say, the absorption of abdominal fat to X-ray increases with the increase of tube voltage under CT imaging. The more abdominal fat content, the greater the measurement error, the greater the impact on the accuracy of measurement.

The technological innovation of fast kilovoltage (KV)-switching dual-energy computed tomography (DECT) has enabled the accurate measurement of vertebral BMD (13-16). The DECT used the hydroxyapatite water (HAP-H_2O) decomposition method, and the main components of European spine phantom (ESP) vertebrae were equivalent to hydroxyapatite (HAP) and water, so the DECT measurements were relatively less affected by abdominal total adipose tissue (TAT). Cui *et al.* (17) showed that 0.8 seconds (s)/rotation (rot), 230 mA, and HAP-H_2O measurements of BMD could further ensure the accuracy of measurement. However, their findings did not consider the effects of abdominal fat and ribs on the vertebral body. Therefore, we simulated the abdominal conditions of normal and obese people using the ESP and aimed to explore the optimal scanning parameters of DECT for accurately measuring BMD and to provide suitable DECT scanning conditions for the human body.

Methods

Phantom

The ESP (QRM GmbH, Moehrendorf, Germany) used in this study (18) consists of an epoxy resin and 3 HAP inserts of densities 50 mg/cm^3 (osteoporosis), 102 mg/cm^3 (osteopenia), and 197 mg/cm^3 (normal), labeled as the first (L1), second (L2), and third lumbar vertebrae (L3), respectively. Different sizes of fresh (within 6 hours after slaughter) porcine-isolated fat (without skin) were selected and wrapped around the ESP to simulate the lower TAT of human with different obesity levels. Then, 6 fresh porcine-isolated ribs (from the slaughterhouse) were selected and wrapped around the ESP and fat diagonally on both sides to simulate the upper TAT of people with different obesity levels.

TAT area measurement

We wrapped 4 pieces of porcine-isolated fat around ESP separately and scanned by QCT protocol using a 256-section rapid KV-switching DECT scanner

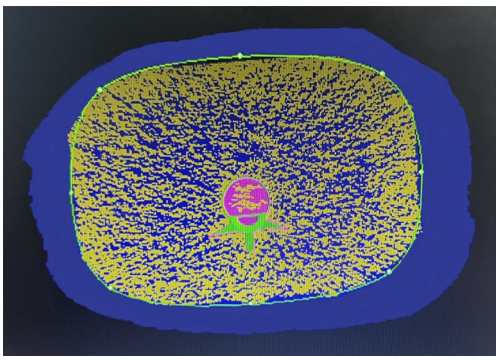

Figure 1 QCT measures the abdominal fat at the central level of the L2. The blue part outside the green aperture is the total abdominal fat. QCT, quantitative computed tomography.

(Revolution; GE Healthcare, Waukesha, WI, USA). The scanning parameters were as follows: tube voltage, 120 kV; tube current, 200–370 mA using automatic milliampere technology; tube speed, 0.8 s/rot; and pitch, 0.984:1. The QCT measurement software is calibrated periodically. The reconstructed 1.25 mm thin-slice CT images were transferred to the QCT workstation (Mindways Software Inc., Austin, TX, USA), and the TAT area at L2 central level was measured using "Tissue Composition Analysis" function (*Figure 1*). The measured areas of 4 porcine-isolated fat were around 140, 240, 340, and 450 cm^2, respectively. TAT =240 cm^2 denoted the average TAT in the lower abdomen of normal weight people; TAT =140 cm^2 + ribs denoted the average TAT in the upper abdomen of normal weight people; TAT =340 cm^2 + ribs denoted the average TAT in the upper abdomen of obese people; and TAT =450 cm^2 denoted the average TAT in the lower abdomen of obese people.

Data acquisition and image reconstruction

GE Revolution 256-slice CT was employed to obtain DECT scans of the phantom (the phantom wrapped in fat/fat + ribs). Air correction was performed before each scan. The phantom was placed in the center of the CT bed with a height of 135 cm. A total of 20 groups DECT scans were performed, namely, tube speed 0.5 s/rot with 5 sets of tube currents (200, 240, 280, 320, and 365 mA); tube speed 0.6 s/rot with 5 sets of tube currents (195, 235, 280, 320, and 360 mA); tube speed 0.8 s/rot with 5 sets of tube currents (190, 230, 275, 315, and 355 mA); and tube speed 1.0 s/rot with 5 sets of tube currents (185, 230, 270, 315, and 355 mA). All other acquisition parameters of DECT were applied as follows: gemstone spectral imaging (GSI) mode with rapid KV-switching between 80 and 140 kVp; helical pitch, 0.984:1; reconstruction slice thickness: 2.5 mm. For each group, 10 scans were conducted, with repositioning after each scan to assess the stability of the measurements and calculate the average value for each group. All reconstructed images were transferred to an advanced image processing station (AW4.7, GE Healthcare, IL, USA). The volume CT dose index (CTDIvol) for each scanning condition was recorded.

BMD value measurement

The measurement of HAP was conducted using fast KV-switching DECT HAP-H_2O decomposition technique on the AW4.7 workstation. The HAP value was chosen to represent the BMD. The measurement was completed by 2 physicians independently. The circular region of interest (ROI) with a size of 20×20 mm was placed at the median level of the vertebral body including as much of the bone cancellous as possible, while avoiding the areas with high BMD, for example, bone cortex and vertebral pedicle. The ROI was measured 3 times and the average value was calculated (*Figure 2*).

Statistical analysis

Statistical analysis were performed using SPSS software version 26.0 (IBM Corp., Armonk, NY, USA). The difference between the measured value of ESP L1–3 vertebral body and the actual value was compared by single sample *t*-test, and the data were in line with normal distribution. Quantitative data were described with $\bar{x}\pm s$ and $P<0.05$ was considered statistically significant. Relative error (RE) was used to evaluate the accuracy of the BMD of each ESP vertebra measured by DECT:

$$RE = \frac{\text{measured value} - \text{true value}}{\text{true value}} \times 100\% \quad [1]$$

Root mean square error (RMSE) of BMD measurements in normal and obese people under different scanning conditions was calculated. The accuracy of scanning mode measurements was evaluated by RMSE as it can reflect the accuracy of the measurement very well. The RMSE is the square root of the ratio of the deviation between the measured value and the true value and the number of

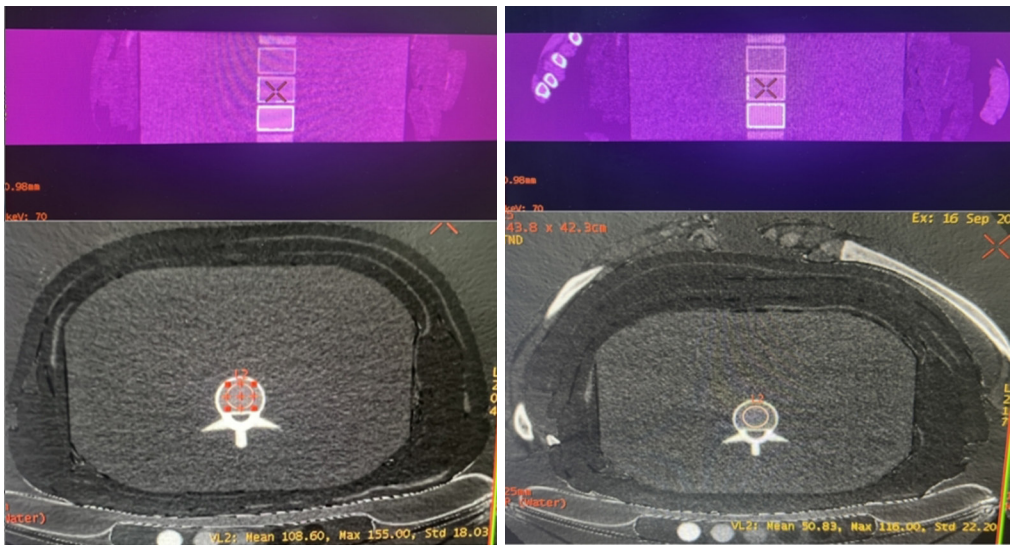

Figure 2 Selected fresh pig fat and fat + rib wrapped around the ESP, CT axial diagram. BMD of the lumbar spine was measured, represented by L2. The middle slice (×) was selected on sagittal CT images. ROI (pink ellipse region) was selected from the corresponding axial CT images, and the sizes were all 20×20 mm. ESP, European spine phantom; CT, computed tomography; BMD, bone mineral density; ROI, region of interest.

measurements (N), achieved with the following formula:

$$RMSE = \sqrt{\frac{\sum_{i=1}^{N}(y_i - \bar{y}_i)^2}{N}} \quad [2]$$

Results

Measurements under each scanning condition in the upper and lower abdomen for different obesity levels are shown in *Tables 1-4*, accuracy under each scanning condition in the upper and lower abdomen for different obesity levels are shown in *Tables 1-4*, and the RMSE of the measurements under each scanning condition in the upper and lower abdomen for different obesity levels are shown in *Figure 3*.

Combining the measurement results and accuracy, RMSE, and radiation dose, the following results were obtained. When simulating the upper abdominal condition (fat area 140 cm^2 with rib influence) in normal weight people, there was no statistically significant difference in BMD measurements of each vertebra for 0.8 s/rot paired with different tube currents (P>0.05), the RE was the smallest for 0.8 s/rot, 190 mA condition (L1: −0.41%, L2: −0.34%, L3: −1.54%), and the RE was the smallest for 190 mA condition had the smallest RMSE for L1 and 2 vertebral BMD measurements (190 mA: L1: 0.69, L2: 1.19); when simulating the lower abdominal condition of a normal-weight population (240 cm^2 of fat area, no rib influence), there was no statistically significant difference between 190 and 275 mA conditions for measurements taken in the 0.8 s/rot, 190 and 275 mA conditions (0.8 s/rot, 190 mA, L1: P=0.17, L2: P=0.06, L3: P=0.78; 275 mA, L1: P=0.12, L2: P=0.69, L3: P=0.28), and 190 mA condition RE was less than that of 275 mA (190 mA: L1: 5.27%, L2: 2.44%, L3: −0.24%; 270 mA: L1: 6.71%, L2: 2.5%, L3: 1.73%), and the RMSE in the 190 mA condition was also less than that in the 275 mA condition (190 mA: L1: 3.46, L2: 2.50, L3: 2.13; 275 mA: L1: 3.81, L2: 4.07, L3: 4.76).

The upper abdomen condition of the simulated obese population (fat area 340 cm^2, affected by ribs), and there was no statistical difference between the measurement results under 0.8 s/rot, 315 and 355 mA conditions (0.8 s/rot, 315 mA, L1: P=0.11, L2: P=0.22, L3: P=0.02; 355 mA, L1: P=0.22, L2: P=0.63, L3: P=0.16), and the RE under 315 mA condition was less than 355 mA (315 mA: L1: 2.71%, L2: −0.76%, L3: −2.61%; 355 mA: L1: 2.79%, L2: 0.87%, L3: −3.66%), and RMSE under 315 mA conditions was also lower than 355 mA (315 mA: L1: 1.52, L2: 0.99, L3: 5.23; 355 mA: L1: 1.78, L2: 2.41, L3: 8.55); at the level of the lower abdomen of the simulated obese population (fat area 450 cm^2, no rib influence), there was no statistical difference in the measurement results under 0.8 s/rot and 315 mA

Table 1 The measured value of DECT under each scanning protocol in the upper abdomen of simulated normal weight population (L1–2 level) and the statistical results between the measured value and the actual value

Rotation time (s/r)	Tube current (mA)	L1 (50 mg/cm^3)			L2 (102 mg/cm^3)			L3 (197 mg/cm^3)		
		HAP	P value	RE	HAP	P value	RE	HAP	P value	RE
Fat area (140 mm^2) + rib cage										
1.0	185	54.96±1.93	0.047	9.93%	109.04±3.28	0.065	6.91%	196.38±1.24	0.477	–0.32%
	230	50.05±1.64	0.963	0.10%	102.10±0.95	0.877	0.09%	195.16±4.81	0.576	–0.93%
	270	54.43±1.15	0.022	8.87%	108.73±2.18	0.033	6.60%	196.96±0.76	0.930	–0.02%
	315	51.53±2.12	0.336	3.07%	103.84±2.42	0.320	1.80%	191.83±4.23	0.168	–2.62%
	355	52.04±2.54	0.299	4.08%	102.40±0.03	0.002	0.39%	191.30±4.12	0.139	–2.89%
0.8	190	49.79±0.80	0.699	–0.41%	101.65±1.40	0.707	–0.34%	193.97±6.93	0.528	–1.54%
	230	49.48±2.12	0.712	–1.04%	102.60±0.05	0.002	0.59%	197.44±4.52	0.883	0.22%
	275	51.73±2.16	0.299	3.47%	103.05±1.39	0.319	1.03%	196.65±1.00	0.604	–0.18%
	315	51.47±4.06	0.595	2.94%	103.48±1.75	0.281	1.45%	194.76±2.83	0.304	–1.14%
	355	50.16±1.00	0.471	0.31%	102.51±0.22	0.057	0.50%	193.43±3.90	0.254	–1.81%
0.6	195	54.03±8.04	0.477	8.05%	101.05±1.60	0.410	–0.93%	204.60±6.70	0.188	3.86%
	235	59.21±5.06	0.088	18.41%	101.61±1.84	0.747	–0.39%	197.41±0.47	0.268	0.21%
	280	57.30±6.88	0.207	14.61%	110.71±3.99	0.063	8.54%	200.27±4.83	0.362	1.66%
	320	57.02±3.85	0.034	14.03%	110.60±1.31	0.008	8.43%	198.00±3.70	0.686	0.51%
	360	61.20±2.83	0.021	22.40%	108.55±6.07	0.203	6.42%	195.34±3.23	0.466	–0.84%
0.5	200	50.76±2.11	0.007	1.53%	102.54±4.50	0.855	0.53%	174.72±11.17	0.075	–11.31%
	240	44.71±3.21	0.039	–10.58%	95.64±8.47	0.323	–6.24%	183.55±9.47	0.133	–6.83%
	280	41.56±1.89	0.011	–16.89%	99.46±0.89	0.039	–2.49%	181.99±7.75	0.079	–7.62%
	320	48.02±0.80	0.032	–3.97%	99.58±2.33	0.214	–2.37%	179.40±4.20	0.018	–8.93%
	365	40.56±5.74	0.745	–18.89%	98.63±3.86	0.270	–3.30%	177.63±8.56	0.059	–9.83%

Data are expressed as mean ± SD. L1, L2, and L3 represent vertebrae of different bone mineral density. Note: 140 mm^2 porcine subcutaneous fat and porcine ribs were selected from the upper abdomen of the normal weight population and wrapped around the ESP; 0.8 s/rot with different tube currents L1, L2, and L3 measurements were not statistically different (P>0.05). The RE (L1: –0.41%, L2: –0.34%, L3: –1.54%) is small at 0.8 s/rot, 190 mA, and the radiation dose is low. DECT, dual-energy computed tomography; HAP, hydroxyapatite; RE, relative error, data are presented as %; SD, standard deviation; ESP, European spine phantom.

conditions (L1: P=0.06, L2: P=0.05, L3: P=0.46). RE at 315 mA was small (L1: 3.75%, L2: –1.06%, L3: 0.42%), and RMSE at 315 mA was also small (L1: 2.13, L2: 1.21, L3: 1.66). With the increase of tube current, the CTDIvol value of the same tube speed increased (*Figure 4*).

Discussion

Currently, QCT and DXA are commonly used to measure BMD. DXA has been widely used in many regions. However, it measures areal (2-dimensional) BMD (aBMD; g/cm^2), whereas QCT measurements focus on vBMD (mg/cm^3) which avoids measurement inaccuracies caused by overlapping projections (19). CT is also a commonly used imaging method for the diagnosis of osteoporosis. In practical work, QCT is mostly carried out simultaneously with clinical routine CT scans without additional radiation dose and scan time. Recently, DECT has become progressively more widespread in clinical application. DECT has the unique ability to differentiate a variety of

Table 2 The measured values of DECT under various scanning protocols in the lower abdomen of simulated normal weight people (L4 level) and the statistical results between the measured values and the actual values

Rotation time (s/r)	Tube current (mA)	L1 (50 mg/cm^3)			L2 (102 mg/cm^3)			L3 (197 mg/cm^3)		
		HAP	P value	RE	HAP	P value	RE	HAP	P value	RE
Fat area (240 mm^2)										
1.0	185	59.96±2.15	0.015	19.91%	111.99±0.74	9.79%	0.046	205.55±2.80	0.034	4.34%
	230	53.97±0.60	0.008	7.95%	107.44±0.95	5.33%	0.037	201.53±2.01	0.060	2.30%
	270	56.08±1.57	0.021	12.16%	106.46±1.24	4.38%	0.045	199.29±1.49	0.117	1.16%
	315	53.30±1.42	0.056	6.59%	104.03±1.66	1.99%	0.242	194.54±0.51	0.014	–1.25%
	355	51.61±1.18	0.141	3.22%	103.16±1.46	1.14%	0.254	190.25±3.54	0.081	–3.43%
0.8	190	52.64±2.75	0.172	5.27%	104.49±0.26	2.44%	0.064	196.52±2.55	0.777	–0.24%
	230	55.94±1.46	0.020	11.87%	107.50±1.37	5.40%	0.102	195.44±2.22	0.348	–0.79%
	275	53.35±2.22	0.120	6.71%	104.55±3.89	2.50%	0.685	200.41±4.07	0.284	1.73%
	315	53.71±0.66	0.010	7.41%	106.47±2.20	4.38%	0.097	195.62±0.63	0.063	–0.70%
	355	54.44±0.78	0.010	8.88%	105.28±1.70	3.22%	0.316	193.62±2.87	0.178	–1.72%
0.6	195	54.20±0.59	0.007	8.39%	106.53±2.13	4.44%	0.282	187.94±1.47	0.009	–4.60%
	235	55.03±2.60	0.078	10.06%	106.76±3.78	4.67%	0.459	190.63±1.37	0.015	–3.23%
	280	50.56±1.55	0.596	1.12%	102.95±2.42	0.93%	0.910	190.19±1.46	0.015	–3.46%
	320	56.52±0.84	0.005	13.05%	106.26±2.40	4.17%	0.038	194.94±3.03	0.360	–1.05%
	360	54.67±3.92	0.175	9.33%	102.93±2.89	0.91%	0.725	194.56±2.11	0.183	–1.24%
0.5	200	60.79±1.61	0.007	21.59%	113.83±5.71	11.59%	0.116	201.98±6.06	0.290	2.53%
	240	54.47±1.58	0.039	8.94%	105.78±0.63	3.70%	0.106	198.65±3.85	0.536	0.84%
	280	53.64±0.66	0.011	7.29%	106.13±3.09	4.05%	0.425	194.63±0.71	0.028	–1.20%
	320	53.51±1.12	0.032	7.01%	104.47±3.76	2.42%	0.763	194.07±5.87	0.478	–1.49%
	365	50.83±3.84	0.745	1.65%	101.60±3.87	–0.39%	0.389	187.50±3.74	0.048	–4.82%

Data are expressed as mean ± SD. L1, L2, and L3 represent vertebrae of different bone mineral density. Note: 240 mm^2 porcine subcutaneous fat was selected from the lower abdomen of the normal weight population and wrapped around the ESP; 0.8 s/rot, 190 and 275 mA conditions were measured without statistical differences (P>0.05). At 0.8 s/rot, RE (L1: 5.27%, L2: 2.44%, L3: –0.24%) at 190 mA was the smallest, and the radiation dose was low. DECT, dual-energy computed tomography; HAP, hydroxyapatite; RE, relative error, data are presented as %; SD, standard deviation; ESP, European spine phantom.

material types, for example, HAP, based on differential X-ray attenuation at different photon energies. Li *et al.* (20) demonstrated that both QCT and DECT can accurately measure BMD while scanning ESP. Cui *et al.* indicated that the combination of 0.8 s/rot tube speed and 230 mA tube current are the optimal DECT scanning parameters, and the basic material pairs (HAP-water) can further ensure the accuracy while measuring BMD. They also showed that DECT can accurately measure vertebral BMD. However, the effect of adipose tissue on the BMD measurement was ignored in this study. In our previous study, we demonstrated that abdominal adipose tissue has a certain effect on the BMD measurement (21). A greater TAT content results in a greater BMD error, thus the accuracy of BMD is limited. Javed *et al.* (22) used DXA to measure the BMD of a bovine femur and found that as the fat layer around the femur increased, the BMD also gradually increased, which suggests that the absorption of

Table 3 The measured value of DECT under each scanning protocol in the upper abdomen of simulated obese population (L1–2 level) and the statistical results between the measured value and the actual value

Rotation time (s/r)	Tube current (mA)	L1 (50 mg/cm^3)			L2 (102 mg/cm^3)			L3 (197 mg/cm^3)		
		HAP	P value	RE	HAP	P value	RE	HAP	P value	RE
Fat area (340 mm^2) + rib cage										
1.00	185.00	56.32±3.98	0.111	12.65%	109.27±2.96	0.051	7.12%	199.32±3.06	0.319	1.18%
	230.00	52.15±4.40	0.486	4.31%	110.92±3.00	0.036	8.74%	195.43±3.53	0.522	–0.80%
	270.00	55.50±4.11	0.146	10.99%	105.86±5.62	0.356	3.78%	198.68±2.51	0.367	0.85%
	315.00	52.38±0.32	0.006	4.77%	101.22±2.04	0.577	–0.76%	194.47±3.02	0.284	–1.28%
	355.00	49.49±2.14	0.721	–1.01%	97.11±3.67	0.147	–4.80%	189.12±2.74	0.038	–4.00%
0.80	190.00	48.15±0.62	0.036	–3.71%	92.46±3.70	0.047	–9.35%	187.61±2.03	0.015	–4.77%
	230.00	56.96±0.88	0.057	13.91%	92.29±10.38	0.247	–9.52%	196.27±11.80	0.925	–0.37%
	275.00	55.66±2.14	0.044	11.32%	97.53±5.00	0.262	–4.39%	189.33±4.55	0.100	–3.89%
	315.00	51.36±0.84	0.107	2.71%	101.22±0.76	0.218	–0.76%	191.85±1.10	0.015	–2.61%
	355.00	51.39±1.36	0.218	2.79%	102.88±2.75	0.634	0.87%	189.79±5.63	0.157	–3.66%
0.60	195.00	45.73±6.01	0.344	–8.53%	85.71±8.92	0.087	–15.97%	195.24±7.86	0.736	–0.89%
	235.00	43.51±0.36	0.001	–12.97%	86.43±5.56	0.040	–15.26%	195.43±11.36	0.834	–0.80%
	280.00	46.31±6.46	0.427	–7.38%	99.53±1.86	0.147	–2.42%	202.62±10.39	0.447	2.85%
	320.00	53.00±2.48	0.171	5.99%	93.78±1.81	0.016	–8.06%	194.22±7.09	0.567	–1.41%
	360.00	55.62±2.97	0.082	11.24%	100.16±2.67	0.356	–1.80%	194.26±5.26	0.462	–1.39%
0.50	200.00	43.84±3.14	0.077	–12.31%	77.84±9.27	0.046	–23.69%	169.70±14.92	0.087	–13.86%
	240.00	38.06±6.94	0.096	–23.88%	87.79±19.72	0.338	–13.93%	178.27±7.58	0.051	–9.51%
	280.00	40.48±4.17	0.058	–19.05%	91.52±2.54	0.019	–10.27%	172.93±8.28	0.037	–12.22%
	320.00	44.70±3.82	0.138	–10.61%	86.83±6.95	0.063	–14.88%	175.99±9.30	0.060	–10.67%
	365.00	43.28±2.56	0.045	–13.45%	85.53±1.18	0.002	–16.15%	181.18±4.70	0.028	–8.03%

Data are expressed as mean ± SD. L1, L2, and L3 represent vertebrae of different bone mineral density. Note: 340 mm^2 porcine subcutaneous fat and porcine ribs were selected from the upper abdomen of the obese population and wrapped around the ESP. At 0.8 s/rot and 315 and 355 mA conditions with no statistical difference in measurement results (P>0.05). At 0.8 s/rot, RE at 315 mA was small (315 mA: L1: 2.71%, L2: –0.76%, L3: –2.61%), and the radiation dose was low. DECT, dual-energy computed tomography; HAP, hydroxyapatite; RE, relative error, data are presented as %; SD, standard deviation; ESP, European spine phantom.

photons by fat gives a spuriously high reading of BMD. Yu *et al.* (11) used DXA and QCT scans of ESP wrapped in different thicknesses of fat layers and found that increasing the thickness of the fat resulted in decreased QCT BMD measurements, forming measurement errors, but with less and more uniform measurement errors compared to DXA BMD measurements. DECT is a scanning method that uses high and low energy switching to measure the BMD of the vertebral body by means of material separation technique. DECT makes the composition of the vertebral body in the body membrane be completely represented by HAP and water, and therefore not susceptible to abdominal fat and other external factors. Ye *et al.* (23) showed that the RMSE measured by both DECT and QCT was positively correlated with the TAT and further indicated that a greater TAT area led to a greater RMSE which suppressed the accuracy of BMD. Therefore, the effect of abdominal fat content should be considered while measuring vertebral

Table 4 The measured values of DECT under various scanning protocols in the lower abdomen of simulated obese people (L4 level) and the statistical results between the measured values and the actual values

Rotation time (s/r)	Tube current (mA)	L1 (50 mg/cm^3)			L2 (102 mg/cm^3)			L3 (197 mg/cm^3)		
		HAP	P value	RE	HAP	P value	RE	HAP	P value	RE
Fat area (450 mm^2)										
1.00	185.00	53.13±5.48	0.378	6.27%	108.14±2.73	0.018	6.02%	191.48±6.06	0.190	–2.80%
	230.00	52.59±0.96	0.009	5.18%	103.58±1.14	0.075	1.55%	193.87±2.94	0.139	–1.59%
	270.00	56.14±2.45	0.012	12.29%	105.87±1.04	0.003	3.79%	195.84±3.6	0.606	–0.59%
	315.00	50.18±0.28	0.340	0.35%	102.17±1.24	0.821	0.17%	185.9±5.98	0.033	–5.63%
	355.00	52.27±0.69	0.008	4.54%	100.79±1.32	0.179	–1.19%	190.51±5.49	0.111	–3.30%
0.80	190.00	52.73±0.65	0.002	5.47%	104.57±1.82	0.070	2.52%	192±3.4	0.064	–2.54%
	230.00	54.81±2.78	0.040	9.61%	102.79±2.34	0.590	0.77%	190.11±2.09	0.005	–3.50%
	275.00	53.55±1.66	0.021	7.10%	104.49±1.95	0.091	2.44%	191.89±5.34	0.173	–2.60%
	315.00	51.87±1.25	0.060	3.75%	100.92±0.67	0.049	–1.06%	197.83±1.76	0.461	0.42%
	355.00	53.62±0.27	0.003	7.24%	101.72±0.03	<0.001	–0.27%	190.9±1.09	0.002	–3.10%
0.60	195.00	50.23±6.28	0.952	0.46%	98.37±3.11	0.114	–3.56%	190.79±5.41	0.118	–3.15%
	235.00	48.29±2.94	0.371	–3.42%	98.59±5.1	0.311	–3.35%	194.42±1.29	0.025	–1.31%
	280.00	49.04±1.79	0.404	–1.93%	99.75±3.07	0.274	–2.20%	189.54±3.66	0.024	–3.79%
	320.00	49.67±3.89	0.891	–0.65%	102.08±4.32	0.976	0.08%	191.3±3.45	0.046	–2.89%
	360.00	53.63±4.67	0.238	7.25%	104.89±0.33	0.000	2.83%	196.77±3.26	0.900	–0.12%
0.50	200.00	57.86±2.7	0.007	15.72%	108.39±1.81	0.004	6.27%	190.39±5.3	0.097	–3.35%
	240.00	66.28±5.05	0.005	32.57%	112.28±4.34	0.015	10.08%	207.19±3.47	0.007	5.17%
	280.00	60.23±4.59	0.018	20.46%	112.55±2.7	0.002	10.34%	197.1±3.65	0.964	0.05%
	320.00	59.12±3.12	0.007	18.23%	110.3±3.85	0.020	8.14%	197.83±4.51	0.767	0.42%
	365.00	48.88±5.19	0.728	–2.23%	93.83±1.62	0.001	–8.01%	177.04±5.75	0.004	–10.13%

Data are expressed as mean ± SD. L1, L2, and L3 represent vertebrae of different bone mineral density. Note: 450 mm^2 porcine subcutaneous fat wrapped around the ESP was selected from the lower abdomen of the obese population, and there was no statistical in 315 mA (P>0.05). At 0.8 s/rot, RE at 315 mA was small (315 mA: L1: 3.75%, L2: –1.06%, L3: 0.42%). DECT, dual-energy computed tomography; HAP, hydroxyapatite; RE, relative error, data are presented as %; SD, standard deviation; ESP, European spine phantom.

BMD using DECT and QCT in patients with severe osteoporosis in clinical practice. Therefore, this study simulated the lower abdominal by wrapping fat around the ESP. Moreover, our preclinical observation indicated that scanning range should include 4–8 ribs while measuring L1 and L2 vertebral BMD and the study showed that ribs had no significant effect on the accuracy of vertebral BMD using DECT (24). Therefore, in this study, 6 fresh porcine-isolated ribs (from the slaughterhouse) were selected and wrapped around the ESP and fat diagonally on both sides to simulate the upper TAT of people with different obesity levels. These studies suggest that the optimal scanning parameters of energy spectrum CT, which were studied by phantom as 0.8 s/rot and 230 mA, and the influence of fat and rib on BMD measurement is not taken into account, the optimal scan parameters will change. Therefore, we simulated various upper and lower abdominal phantoms and explored the optimal scanning parameters to guarantee the accuracy of lumbar spine BMD measurement.

The optimal scanning parameters in our study relate to

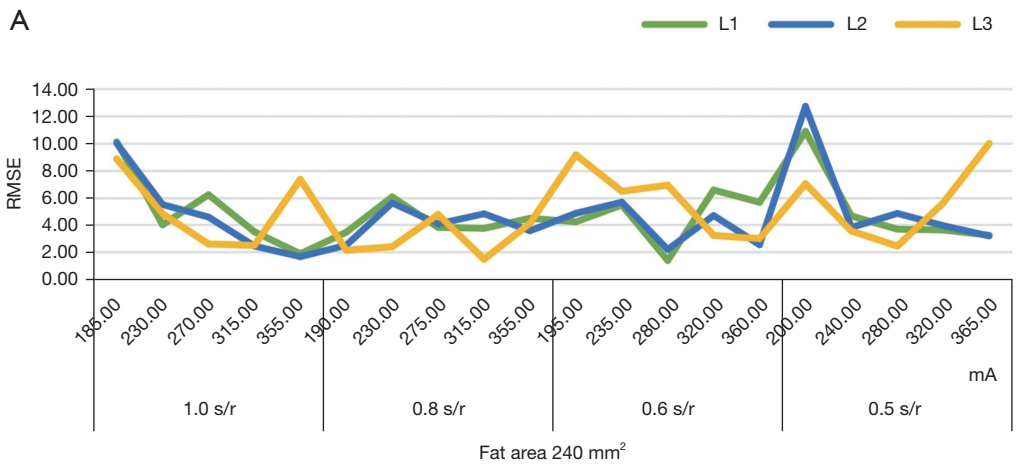

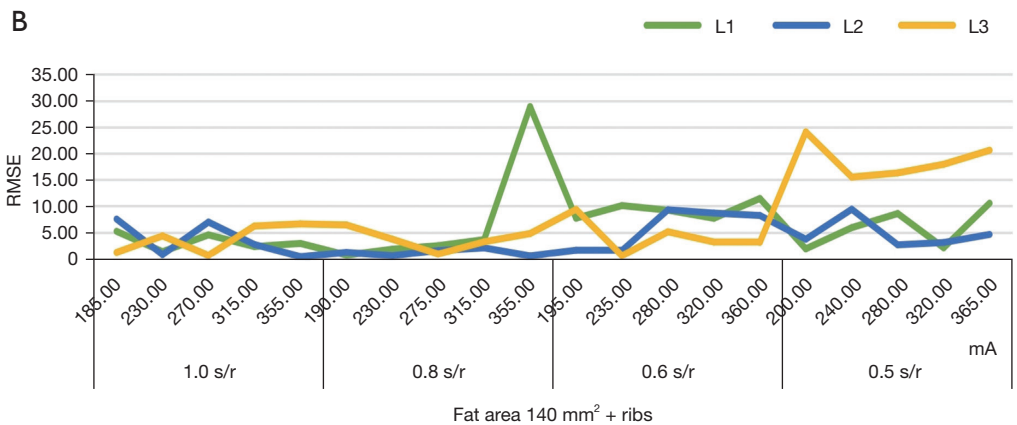

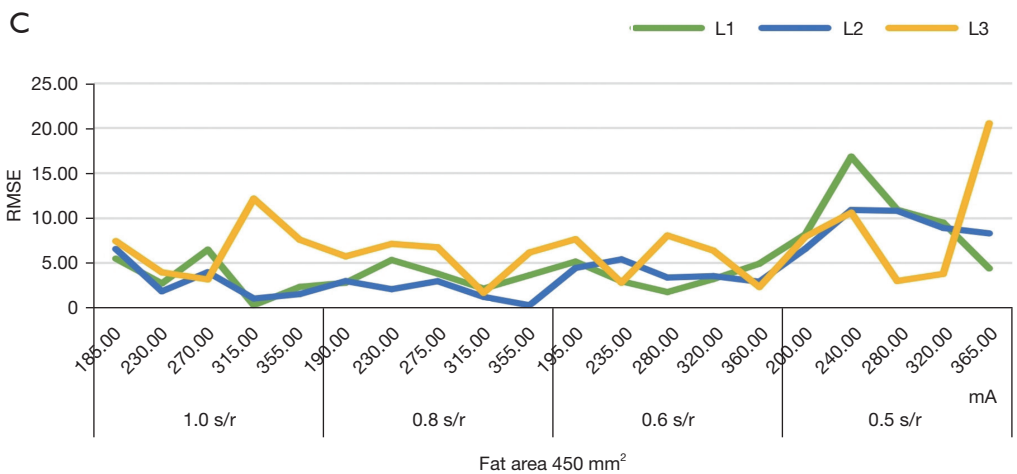

Figure 3 RMSE of BMD measurements under different scanning conditions in normal and obese populations. When simulating the abdomen of normal weight people, L4 level (fat area 240 mm^2, without rib influence condition), 0.8 s/rot, RMSE less than 275 mA under 190 mA condition (190 mA: L1: 3.46, L2: 2.50, L3: 2.13; 275 mA: L1: 3.81, L2: 4.07, L3: 4.76); L1–2 level (fat area 140 mm^2 with rib influence condition), 0.8 s/rot, small RMSE for L1 and 2 at 190 mA condition (190 mA: L1: 0.69, L2: 1.19). When simulating the abdomen of an obese population, at the L4 level (fat area 450 mm^2, without rib influence condition), the RMSE at 0.8 s/rot, 315 mA condition was small (315 mA: L1: 2.13, L2: 1.21, L3: 1.66); at the L1–2 level (fat area 340 mm^2, with rib influence condition), RMSE at 0.8 s/rot, 315 mA condition was less than those at 355 mA (315 mA: L1: 1.52, L2: 0.99, L3: 5.23; 355 mA: L1: 1.78, L2: 2.41, L3: 8.55). RMSE, root-mean-square error; BMD, bone mineral density.

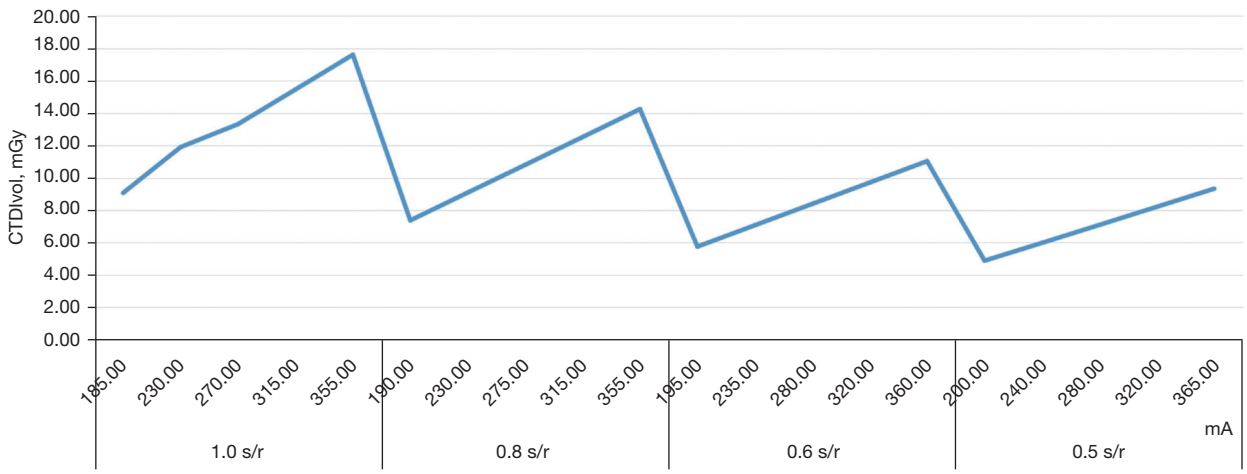

Figure 4 CTDIvol values under different energy spectrum scanning conditions. CTDIvol, computed tomography dose index.

the changes of tube current and rotation speed. We found that two key parameters of CT scanning, namely, tube current and rotation speed, were related to the radiation dose. Radiation dose increases with tube current, and the longer the tube is rotated around, the more information is collected and the higher the radiation dose. In this study, we simulated upper and lower abdominal conditions in normal and obese people and scanned the phantom using the machine's own tube current and rotational speed.

When simulating the upper abdomen of normal weight people, taking into account the two factors of measurement value and RE, it can be seen that the measurement results of

0.8 s/rot with different tube currents are also more accurate. In terms of the optimal dose of radiation, 0.8 s/rot, 190 mA can accurately measure vBMD; in the same way, when simulating the lower abdomen of normal-weight people, 0.6 s/rot, 280 mA RE is lower than 0.8 s/rot, 190 mA, but the radiation dose of 0.8 s/rot, 190 mA is lower, so 0.8 s/rot, 190 mA can be chosen to accurately measure vBMD. In clinical practice, low radiation dose scanning without affecting the accuracy of bone density has become the focus of clinical promotion, under the premise of meeting the needs of image quality in clinical diagnosis, reducing the radiation dose of the recipient, or in the case of the radiation dose cannot be lowered, to maximize the diagnostic imaging information is the direction of clinical efforts. Therefore, we need to reduce the radiation dose while meeting the diagnostic requirements.

The increase of fat area will affect the bone density measurement results, because due to the large area of fat, the absorption attenuation curve of abdominal fat to X-ray shows a bow-back upward behavior, that is, under the condition of CT imaging, the absorption of fat to X-ray is increased with the increase of tube voltage. Ribs are bone structures with a high capacity to absorb X-rays, and thus may affect the measurement results. In contrast, DECT is a scanning method that utilizes high and low energy switching to measure the bone density of the vertebral body using a substance separation technique (12). Meanwhile, energy spectral CT puts the composition within the somatic vertebrae is completely represented by HAP and water, and therefore is less susceptible to external factors such as the rib cage. This study shows that the difference in BMD measured with low mA is statistically significant in the case of 0.8 s/rot, the accuracy and precision of BMD values measured by low mA tube current is low, but the stability is poor, and it is necessary to increase the tube current to more accurately measure the lumbar spine BMD; therefore, for the obese population, the above approach is used for comparison when simulating the conditions of the obese population's upper and lower abdomen, and the selection of 0.8 s/rot, 315 mA can measure vertebral BMD more accurately.

In this study, the precision of energy-spectrum CT was worse than that of QCT, suggesting that current energy-spectrum CT measurements of BMD are slightly less reproducible. The CTDIvol of the GSI partial-scan protocol was higher than that of QCT. The CTDIvol of the DECT was higher than that of QCT; the 0.8 s/rot 190 mA scan protocol, with a lower radiation than that of conventional QCT, reduced the radiation dose without compromising the accuracy of BMD. Energy spectrum CT usually has a high CTDIvol, so it is recommended to use bone density as one of the post-processing methods of clinical energy spectrum CT scanning, not to scan alone.

There are some limitations to this study. First, it was performed using only DECT, and the optimal conditions obtained in this study may not be applicable to other CTs with an energy spectrum. Secondly, it considered the effect of abdominal fat on the measurement of lumbar spine bone density, but the composition of ESP is different from the actual composition of the human vertebrae; therefore, further validation is needed in additional studies. Finally, it did not elucidate the effects of tube rotation speed and tube current on the measurement of BMD by ESP CT.

Conclusions

The results of this study suggest that the use of appropriate scanning parameters allows DECT to correctly measure BMD when the BMD of the material to be measured is within the appropriate range. Taking the radiation dose into account, the condition of 0.8 s/rot 190 mA is recommended for BMD measurement in the case of people with normal weight, and 0.8 s/rot 315 mA is recommended for BMD measurement in the case of obese people.

Acknowledgments

Funding: None.

Footnote

Conflicts of Interest: All authors have completed the ICMJE uniform disclosure form (available at https://qims.amegroups.com/article/view/10.21037/qims-23-1741/coif). The authors have no conflicts of interest to declare.

Ethical Statement: The authors are accountable for all aspects of the work in ensuring that questions related to the accuracy or integrity of any part of the work are appropriately investigated and resolved.

References

1. Rachner TD, Khosla S, Hofbauer LC. Osteoporosis: now and the future. Lancet 2011;377:1276-87.
2. Wu Y, Jiang Y, Han X, Wang M, Gao J. Application of low-tube current with iterative model reconstruction on Philips Brilliance iCT Elite FHD in the accuracy of spinal QCT using a European spine phantom. Quant Imaging Med Surg 2018;8:32-8.
3. Ho CP, Kim RW, Schaffler MB, Sartoris DJ. Accuracy of dual-energy radiographic absorptiometry of the lumbar spine: cadaver study. Radiology 1990;176:171-3.
4. Link TM. Osteoporosis imaging: state of the art and advanced imaging. Radiology 2012;263:3-17.
5. Alawi M, Begum A, Harraz M, Alawi H, Bamagos S, Yaghmour A, Hafiz L. Dual-Energy X-Ray Absorptiometry (DEXA) Scan Versus Computed Tomography for Bone Density Assessment. Cureus 2021;13:e13261.
6. Engelke K, Lang T, Khosla S, Qin L, Zysset P, Leslie WD, Shepherd JA, Schousboe JT. Clinical Use of Quantitative Computed Tomography (QCT) of the Hip in the Management of Osteoporosis in Adults: the 2015 ISCD Official Positions-Part I. J Clin Densitom 2015;18:338-58.
7. Bredella MA, Daley SM, Kalra MK, Brown JK, Miller KK, Torriani M. Marrow Adipose Tissue Quantification of the Lumbar Spine by Using Dual-Energy CT and Single-Voxel (1)H MR Spectroscopy: A Feasibility Study. Radiology 2015;277:230-5.
8. Cheng X, Li K, Zhang Y, Wang L, Xu L, Liu Y, Duanmu Y, Chen D, Tian W, Blake GM. The accurate relationship between spine bone density and bone marrow in humans. Bone 2020;134:115312.
9. Kuiper JW, van Kuijk C, Grashuis JL, Ederveen AG, Schütte HE. Accuracy and the influence of marrow fat on quantitative CT and dual-energy X-ray absorptiometry measurements of the femoral neck in vitro. Osteoporos Int 1996;6:25-30.
10. Bligh M, Bidaut L, White RA, Murphy WA Jr, Stevens DM, Cody DD. Helical multidetector row quantitative computed tomography (QCT) precision. Acad Radiol 2009;16:150-9.
11. Yu EW, Thomas BJ, Brown JK, Finkelstein JS. Simulated increases in body fat and errors in bone mineral density measurements by DXA and QCT. J Bone Miner Res 2012;27:119-24.
12. Aparisi Gómez MP, Ayuso Benavent C, Simoni P, Aparisi F, Guglielmi G, Bazzocchi A. Fat and bone: the multiperspective analysis of a close relationship. Quant Imaging Med Surg 2020;10:1614-35.
13. Sanghavi PS, Jankharia BG. Applications of dual energy CT in clinical practice: A pictorial essay. Indian J Radiol Imaging 2019;29:289-98.
14. Wichmann JL, Booz C, Wesarg S, Kafchitsas K, Bauer RW, Kerl JM, Lehnert T, Vogl TJ, Khan MF. Dual-energy CT-based phantomless in vivo three-dimensional bone mineral density assessment of the lumbar spine. Radiology 2014;271:778-84.
15. Patino M, Prochowski A, Agrawal MD, Simeone FJ, Gupta R, Hahn PF, Sahani DV. Material Separation Using Dual-Energy CT: Current and Emerging Applications. Radiographics 2016;36:1087-105.
16. Woisetschläger M, Hägg M, Spångeus A. Computed tomography-based opportunistic osteoporosis assessment: a comparison of two software applications for lumbar vertebral volumetric bone mineral density measurements. Quant Imaging Med Surg 2021;11:1333-42.
17. Cui X, Huang S, Han H, Yu W. Accuracy and repeatability of Revolution CT energy spectrum imaging in measurement of bone mineral density of spine phantom. Chin J Interv Imaging Ther 2020;17:430-3.
18. Kalender WA, Felsenberg D, Genant HK, Fischer M, Dequeker J, Reeve J. The European Spine Phantom--a tool for standardization and quality control in spinal bone mineral measurements by DXA and QCT. Eur J Radiol 1995;20:83-92.
19. Engelke K, Adams JE, Armbrecht G, Augat P, Bogado CE, Bouxsein ML, Felsenberg D, Ito M, Prevrhal S, Hans DB, Lewiecki EM. Clinical use of quantitative computed tomography and peripheral quantitative computed tomography in the management of osteoporosis in adults: the 2007 ISCD Official Positions. J Clin Densitom 2008;11:123-62.
20. Li X, Li X, Li J, Jiao X, Jia X, Zhang X, Fan G, Yang J, Guo J. The accuracy of bone mineral density measurement using dual-energy spectral CT and quantitative CT: a comparative phantom study. Clin Radiol 2020;75:320.e9-320.e15.
21. Wang Y, Han H, Shi Y, Ye H, Yao N, Yu W. Effect of abdominal adipose content on spine phantom bone mineral density measured by low-mA Quantitative CT. Chin J Osteopor 2023;29:173-8.

22. Javed F, Yu W, Thornton J, Colt E. Effect of fat on measurement of bone mineral density. Int J Body Compos Res 2009;7:37-40.
23. Ye H, Li X, Yao N, Shi Y, Wang Y, Yu W. Effect of abdominal adipose content on spine phantom bone mineral density measured by rapid kilovoltage-switching dual-energy CT and quantitative CT. Quant Imaging Med Surg 2022;12:4914-23.
24. Shi Y, Xing Q, Yao N, Ye H, Wang Y, Yu W. Influence of Ribs on Bone Mineral Density Measurements by Dual-Energy CT and Quantitative CT: a phantom study. Journal of Medical Imaging 2023;33:1449-52.

Cite this article as: Yang Q, Wang Z, Han H, Zhang H, Yu W. Optimal scanning parameters of lumbar bone density measured by fast kilovoltage-switching dual-energy computed tomography (DECT). Quant Imaging Med Surg 2024;14(6):4041-4053. doi: 10.21037/qims-23-1741

